

Electrostatics as the Driving Force Behind the Catalytic Function of the Monoamine Oxidase A Enzyme Confirmed by Quantum Computations

Alja Prah,^{†,‡} Eric Frančišković,^{†,§} Janez Mavri,[†] and Jernej Stare^{*,†}

[†]Theory Department, National Institute of Chemistry, 1001 Ljubljana, Slovenia

[‡]Faculty of Pharmacy, University of Ljubljana, 1000 Ljubljana, Slovenia

Supporting Information

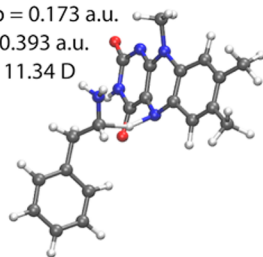
enzyme electrostatics OFF

$\Delta E^\ddagger = 40$ kcal/mol

HOMO-LUMO gap = 0.173 a.u.

charge transfer = 0.393 a.u.

dipole moment = 11.34 D



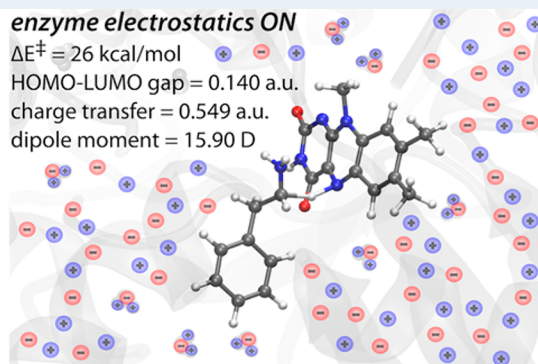
enzyme electrostatics ON

$\Delta E^\ddagger = 26$ kcal/mol

HOMO-LUMO gap = 0.140 a.u.

charge transfer = 0.549 a.u.

dipole moment = 15.90 D



ABSTRACT: While the function of enzymes has been well-known to researchers for decades, the driving force behind it is still a hotly debated topic. Herein, we report significant evidence for electrostatics being that driving force, using a simple, computationally inexpensive, multiscale model of monoamine oxidase A and phenylethylamine. We found that electrostatics provided by the enzyme substantially enhances the reaction by all the considered criteria (lowering the energy barrier, increasing charge transfer, decreasing the highest occupied molecular orbital–lowest unoccupied molecular orbital (HOMO–LUMO) gap, increasing the dipole moment). The catalytic effect can be rationalized by the stabilizing interaction between the dipole moment of the reacting moiety and the electric field exerted by the charged environment. Both the dipole moment and the electric field are perceptibly larger in the transition state as compared to the state of reactants; hence the transition state is stabilized to a larger extent and better solvated than the state of reactants, thereby lowering the barrier. Our findings support the view that catalysis in enzymes originates from preorganized electrostatics.

KEYWORDS: enzyme catalysis, monoamine oxidase, electrostatics, quantum calculations, energy barrier, HOMO–LUMO gap, electric field, dipole moment

1. INTRODUCTION

The indispensable role of enzymes in virtually all life processes has inspired researchers for decades. The paramount role of enzymes is their catalytic function. Enzymes facilitate chemical reactions involved in biological processes to occur at significantly higher rates (and, consequently, at milder conditions) than in the plain aqueous environment. While that feature alone represents an enormous research potential, it should be stressed that enzymes are in every imaginable aspect highly complex systems. Consisting typically of thousands of atoms and including flexible domains, the structure of enzymes is governed by a sophisticated network of interactions, and the formation of the structure (folding) and its stability still remains enigmatic, despite significant research efforts on both the experimental and theoretical fronts. From a theoretical standpoint the complexity of enzymes is reflected, among the rest, in the huge conformational phase space, requiring

dedicated, cutting-edge computing equipment^{1,2} in order to characterize even relatively simple cases of folding dynamics.^{3,4}

The catalytic effect of enzymes is expressed as the increased reaction rate associated with the lowering of the free energy barrier due to the enzymatic environment, typically relative to the aqueous medium. Enzymes are capable of boosting kinetics by several (typically 6–12) orders of magnitude, which corresponds to the barrier lowering of 8–15 kcal/mol.⁵ A typical barrier range of enzymatic reactions is between 13 and 20 kcal/mol, which corresponds to rates on a scale between fractions of a second and minutes.⁶

The driving force behind enzyme catalysis is one of the central questions of chemistry and molecular medicine and has

Received: October 8, 2018

Revised: December 31, 2018

Published: January 2, 2019

long been the subject of profound studies. Pauling suggested, before enzyme structures were available, that the macromolecular environment binds the transition state structure tighter than the reactant structure, giving rise to decreased activation energy.⁷ When enzyme structures became available along with their kinetic and thermodynamic data, the research of enzymatic reactions received strong impetus, which included development of multiscale (quantum mechanics/molecular mechanics (QM/MM)) techniques capable of simulation of enzymatic reactions,^{8–14} thereby supporting the attempts of rationalizing the catalytic function of enzymes.

Several hypotheses on the origin of enzyme catalysis have been proposed and investigated by both experimental and theoretical treatments, but no consensus has been reached to date. The views on this issue can in principle be divided into two major groups, one arguing that the catalytic function derives from *preorganized electrostatics*, and the other suggesting that it is driven by *dynamical effects*. The hypothesis of preorganized electrostatics proposed by Warshel^{15,18} postulates that the polar enzymatic environment stabilizes by electrostatic interactions the transition state (TS) to a larger extent than it stabilizes the state of reactants (R), resulting in barrier lowering (relative to aqueous environment). This concept assumes that the transition state theory is valid for enzymes, the R and TS being in thermal equilibrium, hence Boltzmann statistics takes effect in the TS region. On the contrary, the dynamical effects hypothesis suggests that nonequilibrium effects (beyond the transition state theory) associated with an enzyme's dynamics govern the catalytic power of enzymes.^{19–26} Both views have been (and are still being) vividly debated and critically evaluated by using a wide array of experimental and theoretical techniques, mainly through the aspect of whether or not dynamical effects provide a significant contribution to catalysis, and whether or not the kinetic data can be interpreted through the transition state theory.^{27–34} Several studies suggest that dynamical effects may play a role in the kinetics of enzymatic reactions, but it remains questionable whether these effects are of sufficient magnitude to be decisive for catalysis. The critics of the “dynamical” hypothesis argue that dynamical effects have at best a minor impact on the rates and barriers and cannot account for the massive barrier lowering enforced by enzymes.^{29,30} In line with this criticism, it has been suggested that the coupling of the enzyme modes with the chemical coordinate is not dynamical in its nature.³⁰ On the contrary, promoters of the dynamical concept express the view that (electrostatic) preorganization is a transient, dynamical feature of the enzyme.³⁵

The concept of preorganized electrostatics has recently gained strong research focus, mainly through the role of electric fields in enzymatic reactions and chemical reactivity in general. This has been demonstrated by several examples. In recent efforts toward computationally guided improvements of de novo designed enzymes such as Kemp eliminase enzymes,^{36,37} electrostatics plays a central role, in that optimization of electric fields enhances the stability of the transition state, thereby lowering the reaction barrier. The treatment includes detailed analysis of the electric field at the active site as well as its interaction with dipole moments of chemical bonds involved in the catalyzed reaction.³⁶ It has been demonstrated that by electrostatically guided mutations it is possible to design enzymes with enhanced catalytic power.³⁷ The catalytic role of electrostatics has also been recognized and exploited in other areas of chemical reactivity. The ability to

control chemical reactions by using (external) electric fields has substantial research potential^{38–42} that extends to enzymatic reactions.^{43,44} The efforts in this direction have evolved into a discipline named “electrostatic catalysis”, with promising applications to a variety of reactions.^{45–47} The importance of electric fields for the research of enzymatic reactions also derives from the fact that electric fields in enzymes can be probed experimentally by vibrational Stark spectroscopy.⁴⁸ This is probably the most quantitative experimental measure of electrostatic interactions in enzymes. Recent experimental findings on the role of electric fields in the catalytic function of the ketosteroid isomerase enzyme give strong support for catalysis driven by preorganized electrostatics.⁴⁹ The relevance of electric fields for enzymatic reactions has also attracted the attention of researchers promoting the dynamical concept of enzyme catalysis.⁵⁰ Other recent examples of studies scrutinizing preorganized electrostatics include charge density analysis in the active site of the histone deacetylase 8 enzyme⁵¹ and the electrostatic environment of the catalytic site in monoamine oxidase A and B isoenzymes.⁵²

In view of the motivation to devise proof-of-concept for the driving force behind enzyme catalysis and in line with the increased focus on electrostatics in (enzymatic) reactions, the scope of this work is to augment the existing studies by shedding new light on the catalytic role of electrostatics in enzymes. We use a multiscale computational approach based on the treatment of the reacting moiety by an established quantum chemistry protocol (density functional theory (DFT) in the present case), embedded in the enzymatic environment represented by atomic point charges. While this approach does not account for the interactions within the environment, therefore being unable, for example, to yield meaningful total energy of the entire system or perform molecular dynamics (MD) simulation, it allows for the investigation of the influence of the polar environment on the electronic structure of the reacting subsystem, thereby assessing some vital aspects of reactivity and kinetics. For the electronic wave function such representation is exact, because the electron density interacts with the surroundings exclusively via Coulombic forces. The approach is carried out as single point quantum chemical calculation with external point charges (routinely available in quantum chemistry program packages), and its cost is virtually the same as for the system in the gas phase, even if thousands of point charges are involved. In this way, various quantities related to the reaction can be evaluated, such as reaction barriers, dipole moment, and frontier molecular orbitals, together with the influence of charged surroundings on these quantities. Perhaps the most intriguing aspect of the approach is that one can, at relatively low cost, manipulate with the point charges at will—the charges can be (selectively or entirely) switched off, scaled, displaced, or otherwise modified—giving insight into the role of charged/polar surroundings for the reaction of interest. The herein presented approach of “copying” the partial charges of the protein onto the gas phase quantum calculations in order to account for the electrostatics of the protein was used before in the study of dopamine production catalyzed by CYP2D6, one of the cytochrome P450 enzymes.⁵³

The structures subject to the present approach have to be devised independently (e.g., imported from other simulations). In order to evaluate the catalytic effect of an enzyme, several structures representative of R and TS are required, and these

structures should in principle reflect thermal fluctuations of the reacting moiety and its enzymatic surroundings. A suitable set of structures can be readily obtained from a preceding simulation using one of the established techniques^{54–57} for the sampling of reaction pathways. In the present work we used simulation trajectories acquired by the free energy perturbation approach^{58,59} in the framework of an earlier study.⁶⁰

As the enzyme of interest and its corresponding reaction, we chose monoamine oxidase A (MAO A) and the reactive step of phenylethylamine (PEA) oxidation. Together with the MAO B isoenzyme, MAO A catalyzes the oxidative decomposition of monoamine neurotransmitters in the central nervous system and other tissues, thereby regulating their levels. The function of MAO enzymes is closely related to neurodegeneration and neuropsychiatric disorders.^{61–65} While primary MAO substrates are dopamine, serotonin, and noradrenaline, PEA is an endogenous neuromodulator exhibiting various neurological effects^{66–68} and a popular research substrate of MAO enzymes.^{69–72} Independently of the substrate, the reactive step of decomposition includes the cleavage of the C–H bond vicinal to the amino group accompanied by the transfer of hydrogen atom to the flavin adenine dinucleotide (FAD) prosthetic group present in the active site of the enzyme. In agreement with the assumed hydride transfer mechanism (see the [Supporting Information](#), section S1),^{73,74} the reactive step features negative charge transfer from PEA to FAD.

The present study scrutinizes the electrostatic effects of the protein on the active site, particularly the influence of the macromolecular environment on charge distribution within the reactive subsystem, the pertinent highest occupied molecular orbital–lowest unoccupied molecular orbital (HOMO–LUMO) gap, and the reaction barriers. In addition, we validate the above-described approach and rationalize the catalytic function of MAO A by considering the interaction between the electric field exerted by the solvated enzyme and the dipole moment of the reacting moiety projected onto the presumed direction of the electron flow, in a similar manner as has been recently demonstrated by Head-Gordon and co-workers.^{36,37} The convenience of using these quantities derives from the simplicity at which the free energy of interaction between a dipole and an electric field can be evaluated, together with its impact on the reaction barrier (see the [Supporting Information](#), section S3). Importantly, in this representation the effect of enzyme electrostatics on the barrier can be analyzed at the residue level.

2. COMPUTATIONAL DETAILS

The reacting moiety, consisting of PEA and the flavin ring system of the FAD prosthetic group truncated to the lumiflavin molecule (LFN), was treated by DFT calculations, whereas the environment (solvated protein) was represented by point charges. The state of reactants (R) and the transition state (TS) of the fluctuating system were sampled by taking, for both R and TS, 100 snapshot structures from our previous simulation of the rate-limiting step of PEA oxidation catalyzed by MAO A.⁶⁰ That simulation included classical treatment and facilitated the conversion of reactants to products by using the established free energy perturbation (FEP) methodology,^{58,59} the free energy profiles were computed by the empirical valence bond protocol.^{8,75,76} The model was based on a spherical simulation cell with a radius of 30 Å, centered at the reacting moiety in the active site of MAO A, encompassing the

entire protein and 1884 water molecules (see the [Supporting Information](#), section S2). The simulation was carried out as 10 independent replicas, totaling in 51 ns of MD. For each replica, the snapshot sampling rate within the relevant FEP step was 10 ps. It should be noted that overall the 100 snapshots are not entirely time-resolved between each other. Snapshots corresponding to R and TS are typically separated by ~2.5 ns of MD. The reader is referred to ref 60 for a detailed description of the methods used in that work.

The structures representative of R and TS were identified from the free energy profiles.⁶⁰ For each of the snapshots, the energy and electronic structure (including the dipole moment) were computed for the PEA···LFN reacting moiety (51 atoms, see [Figure S1](#)) at the M06-2X/6-31G+(d,p) level of theory in the gas phase, in the polarizable conductor continuum solvation model (CPCM)^{77,78} representing aqueous medium, and in the presence of 13 898 point charges representing the surroundings provided by the solvated protein. The computed energy was corrected for the Coulombic self-energy of the surrounding charges. The electronic structure was analyzed by the Natural Bond Orbital v. 3.1 (NBO) method,⁷⁹ yielding atomic charges within the reactive subsystem; in addition, atomic charges were also computed by fitting to the electrostatic potential according to the Merz–Kollman (MK) scheme.⁸⁰ Analysis of the HOMO–LUMO gap pertinent to the reaction was done by separately treating the PEA and LFN molecules in the same point charge environment. While the HOMO energy was taken directly from the single point calculation of PEA, the LUMO energy was approximated as the negative of the electron affinity, that is, the energy difference between the neutral LFN molecule and its radical anion. All quantum calculations were carried out by the Gaussian 09 program package.⁸¹ Visualization and analysis of snapshots was carried out by the VMD program.⁸²

Point charges representing the solvated enzyme were taken with their original values, but were also scaled by various factors between –1 and +2, or completely switched off, resulting in a gas-phase model of the reaction. In addition, the effect of electrostatics provided by the environment was studied by limiting the point charges included in the model to selected distances ranging between 5 and 25 Å from the reacting N5 atom of LFN. It should be noted that manipulation with the surrounding point charges represents the only difference between the models; in all other aspects (snapshot geometries, quantum chemistry, etc.) the models are identical.

For each snapshot the electric field exerted by the point charges was evaluated at the midpoint of the C···N vector of the reacting moiety by using the fundamental expression given in the [Supporting Information](#) (section S3). The electric field vector was dot-multiplied by the dipole moment vector of the reacting moiety projected onto the C···N line (presumed direction of the electron flow) to yield the free energy of the electrostatic interaction between the reacting moiety and enzymatic surroundings. This interaction was further analyzed by contributions of individual residues.

3. RESULTS AND DISCUSSION

3.1. Electrostatic Environment Lowers the Barrier.

The reaction barrier, defined as the difference in average energy between the snapshot structures representing the transition state (TS) and the state of reactants (R), exhibits significant dependence on the electrostatic environment

provided by the solvated enzyme. In the absence of charged environment (i.e., in the gas phase) the energy barrier amounts to 40.31 kcal/mol. On inclusion of the point charges representing the protein the barrier drops to 26.09 kcal/mol, as shown in Figure 1. The electrostatic environment stabilizes both R and TS, but the latter is stabilized to a larger extent.

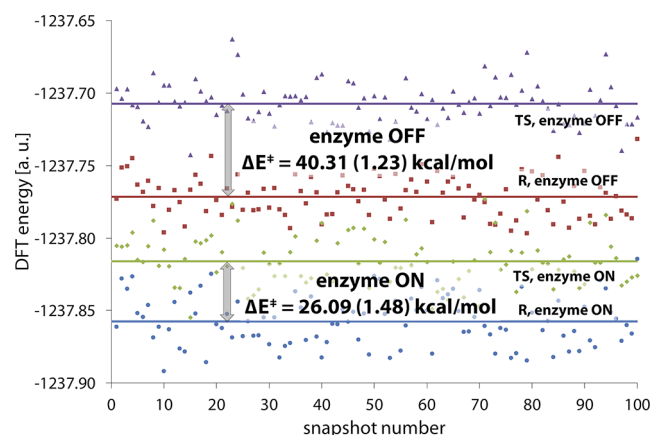


Figure 1. Derivation of the energy barrier from snapshots corresponding to the state of reactants (R) and to the transition state (TS), with point charges representing the enzyme switched on and off. The colored horizontal lines indicate the energies of the corresponding sets averaged over the 100 snapshots, and the energy barrier with the standard error of the mean (SEM) in parentheses is displayed for enzyme electrostatics switched on and off.

The resulting barrier lowering of 14.22 kcal/mol is statistically significant—the corresponding standard error of the mean (SEM) is 1.92 kcal/mol—and can undoubtedly be attributed to electrostatic interactions. As can be seen below, the statistical significance of the effect of electrostatic surroundings holds for all quantities considered in this study. In agreement with earlier studies,^{73,74,83} the barrier lowering corresponds to about 10 orders of magnitude speedup of the reaction rate relative to the gas phase. Note that the present barrier values are apparently overestimated by about 8 kcal/mol, which is rationalized by the slight mismatch between the force field used in the simulation from which the snapshots were taken and the presently used model quantum chemistry. In part, the overestimated barrier may also be attributed to the chosen functional (see the Supporting Information, section S4, for details).

It should be noted that the presented barrier lowering corresponds to using gas phase as the reference state. However, since aqueous reference state is most often used for the interpretation of catalytic effect of enzymes, we also used a continuum solvation model instead of a gaseous reference state, yielding the barrier of 37.01 kcal/mol for the uncatalyzed reaction and the corresponding barrier lowering of ~11 kcal/mol. Therefore, the substantial catalytic effect is conserved regardless of the reference state used in the present approach.

3.2. Electrostatic Environment Enhances Charge Transfer and Increases Dipole Moment. Along with the energy barrier we monitored the effect of electrostatic environment on the charge transfer between PEA and LFN on passing from the R to the TS stage. Charge transfer was estimated by two established methodologies of population analysis (NBO and MK) imposed on the snapshots, as listed in Table 1.

Table 1. Amount of Negative Charge Transfer from PEA to LFN on Passing from the State of Reactants to the Transition State^a

methodology	enzyme OFF	enzyme ON
NBO	0.393 (0.011)	0.549 (0.012)
MK	0.271 (0.009)	0.447 (0.011)

^aThe charge transfer (in atomic charge units, with SEM values in parentheses) is computed as the difference between the sum of atomic charges on PEA in the transition state and in the state of reactants and averaged over 100 snapshots, with point charges representing the enzyme switched on and off. Atomic charges were computed by two distinct methodologies (NBO and MK; see Computational Details).

Inclusion of the electrostatic environment provided by the enzyme noticeably increases the amount of transferred charge (by 0.16–0.18 charge unit). As suggested by various studies,^{73,74,84–87} the reaction between PEA and LFN includes negative charge transfer from PEA to LFN; therefore, the increased charge transfer stimulated by the electrostatic environment reflects enhancement of the reaction. Worth noting, for every single snapshot structure the charge transfer increases when enzyme electrostatics is turned on, further supporting the catalytic role of the charged environment.

The enhanced charge transfer is consistent with the substantial increase of the dipole moment of the reacting moiety on inclusion of the electrostatic environment (Table 2).

Table 2. Dipole Moment of the PEA⋯LFN Reacting Moiety in the State of Reactants (R) and in the Transition State (TS)^a

	enzyme OFF	enzyme ON
R	10.62 (0.06)	14.34 (0.08)
TS	11.34 (0.06)	15.90 (0.09)
difference TS – R	0.72 (0.08)	1.56 (0.12)

^aThe dipole moment (given in debyes, with SEM values in parentheses) was computed at the M06-2X/6-31+G(d,p) level of theory and averaged over the corresponding 100 snapshot structures, with point charges representing the enzyme switched on and off.

The environment causes strong additional polarization, raising the dipole moment by 35 and 40% for R and TS, respectively. Importantly, the increase is larger for the TS and the difference in the dipole moment between R and TS more than doubles on inclusion of enzyme's electrostatics, rendering the TS more susceptible for the interaction with the charged surroundings. This is in agreement with the fundamental feature of chemical reactions, namely that their TSs are more polarizable than the respective reactant and product (P) states and that the TSs possess a larger share of excited (ionic and charge transfer) electronic states relative to R and P, making them prone to large bond ionicity changes and, consequently, more susceptible to external electric fields.⁴² As will be shown in section 3.5, this feature appears to be important for rationalizing the catalytic effect of MAO A.

3.3. Electrostatic Environment Narrows the HOMO–LUMO Gap. We considered frontier molecular orbitals pertinent to the reaction. For the present reaction the characteristic molecular orbitals are the HOMO orbital of PEA and the LUMO orbital of LFN. The energy gap between these orbitals reflects reactivity between PEA and LFN. The gap varies with the geometry of the PEA⋯LFN complex and is

evidently susceptible to the charged environment, as shown in Figure 2.

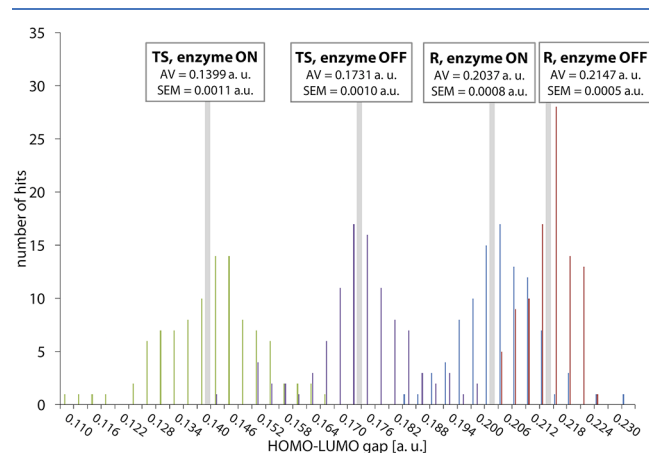


Figure 2. Distribution of the energy gap between the HOMO orbital of PEA and LUMO orbital of LFN (as approximated from the electron affinity) calculated for the snapshots corresponding to the state of reactants (R) and the transition state (TS), with point charges representing the enzyme switched on or off. Average values of the HOMO–LUMO gap are displayed as vertical gray bars, with averages (AV) and standard error of the mean (SEM) also given numerically.

The HOMO–LUMO gap narrows on inclusion of enzyme electrostatics for snapshots corresponding to both R and TS. In the case of reactants, the gap is larger and less sensitive to the charged environment; however, the decrease of ~ 0.01 au is perceivable. When the reacting system is close to the transition state geometry, the HOMO–LUMO gap substantially decreases, and is much more susceptible to the charged environment, decreasing from 0.173 to 0.140 au (by over 20%) on inclusion of enzyme’s electrostatics. This further confirms that the charged environment provided by the enzyme enhances the reactivity.

The reaction-enhancing effect of the enzyme’s electrostatics has been further investigated by manipulation with the point charges representing the enzyme. Manipulations include scaling of the charges (see the [Supporting Information](#), section S5), restricting the charges included in the model up to a selected distance from the reacting moiety, and improper embedding of the reacting moiety into its surroundings. As explained below, results of these manipulations unequivocally demonstrate the significance of electrostatic interactions for the catalytic function of MAO A.

3.4. Distance Cutoff of Charged Environment: At Least 10 Å Required for Convergence. Since electrostatics is a long-range interaction (Coulombic energy decreasing with the inverse of the distance), it can be assumed that, rather than just by the nearest surroundings, the reaction barrier is influenced by a substantial domain of the environment. Also, larger variations of the barrier are expected when small regions of the charged environment are included in the model. Indeed, when considering only the charges within 5 Å from the reacting moiety, the barrier of 35.17 kcal/mol is closer to the one in the gas phase than to the one computed for the full protein environment (Figure 3), demonstrating that such a narrow region cannot account for the effect of the entire environment. When a 7.5 Å shell is considered, the barrier drops to 17.58 Å, indicating that the catalytic effect has been severely overestimated. This possibly reflects not only the

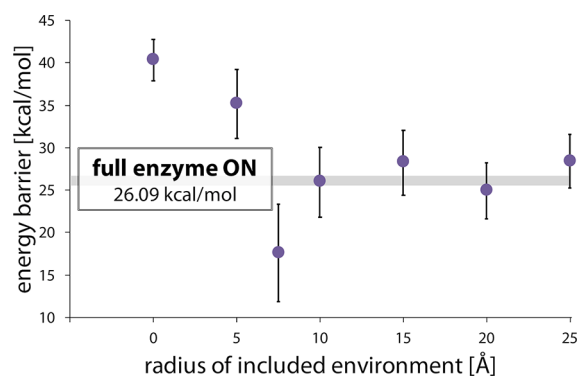


Figure 3. Energy barrier (with error bars representing 95% confidence interval (CI)) as a function of the size (radius) of the spherical domain of the included charged environment. Note that the “full enzyme” notation corresponds to a model with a radius of approximately 30 Å.

insufficiently sized domain of the environment, but also the issue whether individual residues are entirely included in the region or they are “broken” by its border. However, when this region is extended out to 10 Å and more, the barrier stabilizes and fluctuates only slightly around the value of 26.09 kcal/mol obtained for the fully sized model extending to ~ 30 Å from the reacting moiety. It can be estimated that in the present case the inner region of ~ 10 Å provides the majority of the catalytic effect of the charged environment. While further testing is required to generalize this feature to other enzymes, it is worth noting that for practical reasons electrostatic interactions are often subject to a comparable distance cutoff in classical molecular dynamics simulations, suggesting that the present model is reasonable.

3.5. Catalytic Effect Rationalized by Electric Field and Dipole Moment. One of the manipulations with the surroundings was placing two opposite large charges at either side of the reacting moiety. The resulting changes in the barrier appear to be in accordance with the simplified view of the charge distribution in the TS. For instance, when placing a large negative charge closer to PEA and the positive countercharge closer to LFN, the barrier is reduced, and vice versa (see the [Supporting Information](#), section S6). This led us to consider the interaction between the reacting moiety and its enzymatic surroundings by representing the former by its dipole moment vector, and by modeling the influence of the latter with the electric field exerted by the point charges at the midpoint of the C \cdots N moiety of the PEA \cdots LFN complex (Figure 4). The free energy of the interaction between the dipole moment and the electric field (G_{elec}) and the influence of this interaction on the barrier ($\Delta G_{\text{elec}}^{\ddagger}$) can be evaluated trivially (see the [Supporting Information](#), section S3). Since the overall dipole moment vector of the PEA \cdots LFN complex is not aligned with the direction of the electron flow associated with the reaction (also denoted as “reaction axis”⁴²), we considered its projection onto the vector defined by the C atom of PEA and N atom of LFN, because this appears to be crucial for rationalizing the catalytic effect (see Figure 4). Table 3 lists the magnitude of the dipole moment and electric field vectors projected onto the C \cdots N line of the reacting moiety (x), and the corresponding free energies of their interaction, for both R and TS.

When passing from R to TS, the dipole moment component parallel to the reaction axis is not only significantly enlarged,

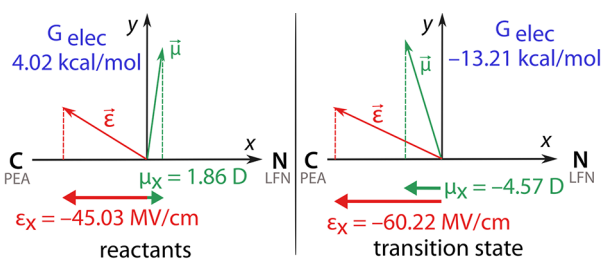


Figure 4. Vectors of the dipole moment (green) and the electric field (red) exerted by the enzyme at the C...N midpoint of the reacting moiety, in the state of reactants and in the transition state. Bold arrows represent the projection of both vectors onto the C...N line ("reaction axis"), marked with x . The corresponding interaction free energy is displayed in blue both for R and for TS.

Table 3. Magnitude of Dipole Moment of the PEA...LFN Reacting Moiety and Electric Field Exerted by the Enzyme's Point Charges on the Reacting Moiety in the State of Reactants (R) and in the Transition State (TS)^a

	R	TS
dipole moment [D]	1.86	-4.57
electric field [MV/cm]	-45.03	-60.22
$G_{\text{elec}}(x)$ [kcal/mol]	4.02	-13.21
$\Delta G_{\text{elec}}^{\ddagger}(x)$ [kcal/mol]		-17.23

^aBoth the dipole moment and the electric field vector are projected onto the C...N line of the reacting moiety (see Figure 4). Values are averaged over 100 corresponding snapshots. The average free energy of interaction between the dipole moment and the electric field (G_{elec}) is also listed. The difference in this quantity between TS and R ($\Delta G_{\text{elec}}^{\ddagger}$) represents the barrier change due to electrostatic interactions along the direction of the electron flow (x).

but also switches its direction, rendering interaction with the electric field from repulsive to attractive. In turn, the corresponding component of the electric field enlarges by about one-third in the TS. Consequently, while R is destabilized due to electrostatic interactions by 4.02 kcal/mol, TS is stabilized by 13.21 kcal/mol, yielding the barrier lowering estimate ($\Delta G_{\text{elec}}^{\ddagger}(x)$) of 17.23 kcal/mol. The agreement with the DFT-computed barrier lowering of 14.22 kcal/mol (section 3.1) can be declared as very reasonable, given the fact that the dipole–electric field model disregards the size of the reacting moiety, mapping all its charge distribution to the corresponding dipole moment vector component. In addition, the C...N midpoint as the probing point for the electric field has been chosen arbitrarily, but the electric field exerted by the enzyme varies in space. Nevertheless, the good qualitative match in the barrier lowering between the two approaches suggests that the presently introduced model is reasonable, confirming that electrostatics represents an important source of the catalytic function of MAO A.

The treatment based on the projection of the net dipole moment of the PEA...LFN complex onto the C...N line has been augmented by approximating the dipole moment with a trivial two-point expression using NBO charges (derived from the DFT density) of the aforementioned C and N atoms, yielding $\Delta G_{\text{elec}}^{\ddagger}(x)$ of -12.65 kcal/mol (Supporting Information, section S9). Such variations between the models can be expected given the undertaken approximations, suggesting that their agreement is reasonable, thereby validating the presently used treatments.

The use of projected dipole moments also allows for the assessment of the component of the dipole moment perpendicular to the presumed electron flow. In contrast to the parallel component, the use of the perpendicular component yields a $\Delta G_{\text{elec}}^{\ddagger}(y)$ value of -2.74 kcal/mol, i.e., a nearly order of magnitude smaller (but still catalytic) contribution (see the Supporting Information, section S8). This clearly indicates that the direction of the electron flow is crucial for the assessment of enzyme catalysis, thereby supporting the standpoint presented in previous related studies.^{36,37,42}

The enhanced electrostatic stabilization of the TS implies that the environment is capable of adapting to the increasingly polar reacting moiety. This was examined by computing the barrier by embedding the reacting moiety into the point charge surroundings improperly, i.e., by combining the reacting moiety in the state of reactants with the surroundings corresponding to the transition state, and/or vice versa (see the Supporting Information, section S7). In all such cases, the barrier increases noticeably, giving evidence that fluctuations of the structure of the enzyme facilitate enhanced stabilization of the TS (as compared to R), making it possible to substantially reduce the reaction barrier.

3.6. Influence of Electrostatics Analyzed by Residue.

Since the electric field exerted by the charged surroundings can be broken down to contributions of individual residues and water molecules, the same can be done for the corresponding barrier change ($\Delta G_{\text{elec}}^{\ddagger}$). The list of $\Delta G_{\text{elec}}^{\ddagger}$ of all residues is given in the Supporting Information (section S10) and displayed in Figure 5 as a function of the distance from the

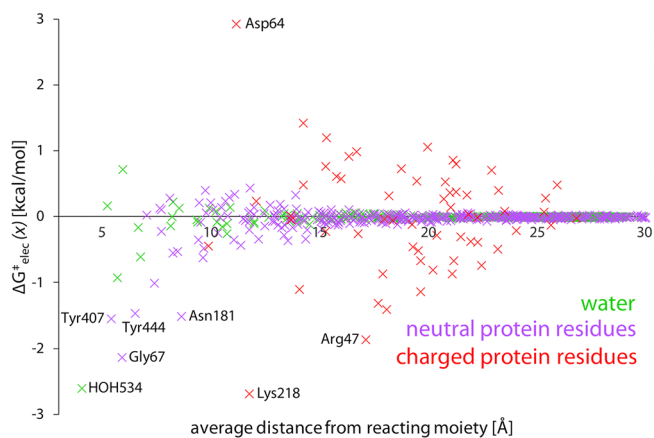


Figure 5. Contribution to the barrier change ($\Delta G_{\text{elec}}^{\ddagger}(x)$; see Table S4) calculated for individual MAO A residues (neutral residues, purple symbols; charged residues, red symbols) and water molecules (green symbols) on the basis of interaction between the dipole moment of the reacting moiety and the electric field exerted by the corresponding residue or water molecule, as a function of the average distance from the reacting moiety. Note that a negative value of $\Delta G_{\text{elec}}^{\ddagger}(x)$ represents catalytic effect, and vice versa for a positive value. Contributions of selected residues are marked with the residue name and number.

reacting moiety. For the entire solvated protein $\Delta G_{\text{elec}}^{\ddagger}$ amounts to -17.23 kcal/mol (Table 3), of which protein residues contribute -12.37 kcal/mol while water molecules provide about 60% smaller contribution, -4.86 kcal/mol. Both contributions are catalytic.

Slightly less than one-tenth of protein residues have a sizable contribution (at least ± 0.4 kcal/mol), and the contribution of these residues to $\Delta G_{\text{elec}}^{\ddagger}$ reaches about 75% of the total contribution of the residues. Most of the charged residues present in the enzyme fall into this group. A significant majority of the residues have only little electrostatic influence, and their net effect is small, but still catalytic (-2.96 kcal/mol).

As expected, the contribution of an individual residue is in general larger when a residue is charged and/or located close to the reacting moiety. As a general rule, the contribution diminishes with the increasing distance from the active site, but the decrease is considerably less pronounced with the charged residues, which is in agreement with the long-range nature of electrostatics. The largest contributions to the changed barrier assume values between ± 1.5 and ± 2.5 kcal/mol, which is about 10% of the total effect. Among residues with the largest contributions most are of catalytic nature (negative $\Delta G_{\text{elec}}^{\ddagger}(x)$), for instance Gly67, Arg47, Lys218, Tyr407, and Asn181, whereas anticatalytic ones such as Asp64 are fewer in number (Figure 5). In agreement with earlier studies, residues of the “aromatic cage” (Tyr407 and Tyr444) with a presumed role in substrate binding and catalysis⁸⁸ exhibit a sizable catalytic effect.

In contrast to protein residues, most of the water molecules provide vanishingly small contributions to the changed barrier, especially if they are farther from the active site than ~ 13 Å. However, few water molecules in the active site exhibit substantial electrostatic influence. The water molecule located closest to the reacting moiety (HOH534, Figure 6) provides a

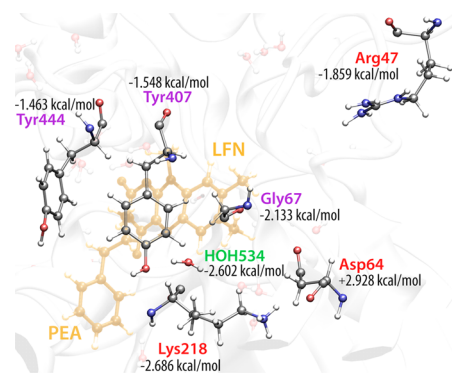


Figure 6. Active site of MAO A with reacting phenylethylamine (PEA) and lumiflavin (LFN) moiety shown in shaded yellow, together with selected residues exhibiting largest (catalytic or anticatalytic) influence on the reaction barrier, with their actual contributions to the barrier indicated.

contribution of -2.60 kcal/mol, exceeding almost all individual contributions of protein residues and amounting to more than half of the net effect of all water molecules. Given that this water molecule remains in the close vicinity of the reacting moiety for at least 100 ns, it can essentially be regarded as part of the active site; similar holds for a few other water molecules in or near the active site. In contrast to water molecules, the contribution of protein residues to $\Delta G_{\text{elec}}^{\ddagger}$ diminishes at a significantly slower pace; however, beyond ~ 25 Å the residues have almost no influence on this quantity.

The analysis of residue contributions to $\Delta G_{\text{elec}}^{\ddagger}(x)$ suggests that the catalytic effect of the charged enzymatic environment of MAO A is very complex and cannot be attributed to just a few selected residues. Not surprisingly, the majority of

electrostatic influence originates from $\sim 10\%$ of the residues which are either polar or charged or located close to the active site. Besides that, the catalytic effect includes a noticeable contribution of a few water molecules present at or near the active site.

4. CONCLUSIONS

We investigated the role of electrostatic interactions in the catalytic function of the MAO A enzyme, by using a simple and affordable yet efficient approach based on embedding the reacting moiety, treated by conventional quantum chemistry protocols, into the enzymatic environment represented by atomic point charges. The structures subject to this approach were extracted from our previous classical simulation of a typical reaction catalyzed by MAO A, namely phenylethylamine oxidation.

We found that the enzymatic environment substantially lowers the reaction barrier, enhances charge transfer during the reaction, decreases the HOMO–LUMO gap, and increases the polarization of the reacting moiety. At the same time, the electric field exerted by the enzyme in the transition state is significantly larger and better aligned with the dipole moment than in the state of reactants. Consequently, the transition state is stabilized to a larger extent than the state of reactants, and the barrier is reduced. This has been verified by the simplified but established approach based on the free energy of interaction between the dipole moment and electric field vectors projected onto the line defined by the C···N atoms of the reacting moiety, which is a presumed direction of the electron flow during the reaction;^{36,37} the estimated barrier lowering of ~ 17 kcal/mol is in good qualitative agreement with the lowering of ~ 14 kcal/mol obtained by the present treatment (~ 11 kcal/mol when using the aqueous reference state).

The present results unequivocally support the importance of electrostatics in reactions catalyzed by MAO A. The estimated magnitude of barrier lowering suggests that the contribution of electrostatics is not only significant, but rather essential for catalysis. While extension of the present approach to a diverse array of enzymes, their substrates, and reactions is required to generalize this statement, the present findings on MAO A are in full agreement with the hypothesis that enzyme catalysis derives from preorganized electrostatics;^{5,16,29,30,76} i.e., enzymes are evolutionarily designed in such a way that they, by electrostatic interactions, provide a more substantial stabilization of the transition state relative to the state of reactants, which is reflected in the lowering of the free energy barrier and in the significantly increased reaction rates. The reasonably explained catalytic effect of the MAO A enzyme through the concept of electrostatics suggests possible extensions of the present approach and its application to the recently proposed computationally driven design of improved enzymes based on the electric field.^{36,37,44} However, it should be noted that, as demonstrated previously, electric field in an enzyme is not necessarily optimized for the catalyzed reaction, but rather for the entire catalytic cycle of the enzyme.^{42,53} Still, the paramount role of electrostatics in enzymes is sustained in such cases.

The role electrostatic forces play in enzymes has also been investigated by experimental probing of electric fields in active sites by using Stark vibrational spectroscopy.^{89–91} The electric field values calculated in this study are reasonably similar to the values experimentally obtained for ketosteroid isomerase

(KSI).⁴⁹ The magnitude of the electric field at the active site of wild-type KSI was found to be -144 ± 6 MV/cm, which is roughly twice as large as the calculated values for MAO A in the present study.

It should be noted that the present approach is not capable of elucidating the potential role of dynamical effects, which constitute another popular hypothesis of the origin of catalysis in enzymes, as proposed by various authors. Investigation of nonequilibrium dynamical effects, i.e., motions within the enzyme facilitating the crossing of the barrier while disobeying Boltzmann statistics, is clearly beyond the reach of the present treatment. Therefore, while supporting the concept of electrostatics, the present study gives no evidence either in favor of or against the dynamical effects in enzymes.

The major advantage of the present approach is that it facilitates studies of the effects of polar/charged environment on the reacting moiety directly at the electronic structure level, since for the electronic wave function this approach is exact. Additionally, the treatment allows for computationally inexpensive but interpretation-rich manipulations with the environment, such as switching the charges off, cutting them off by distance, scaling them, etc.

A few caveats should also be stressed. The herewith reported approach is in essence a reduced version of the electrostatic embedding method in traditional QM/MM techniques, hence lacking dispersion effects on the barrier. In addition, the present treatment does not fully account for the barrier and its lowering on the free energy scale. While thermal averaging has been considered by taking several snapshots representative of reactants and of the transition state, entropy effects have not been entirely included. The omission of entropic effects originating from the system as a whole may be particularly critical when considering contributions of individual residues to catalysis. Therefore, we prefer to denote the barrier as potential energy (ΔE^\ddagger) rather than as free energy, but this is a debatable choice. We made an exception in our notation for the interaction between the dipole moment and the electric field (G_{elec}) for which we used the free energy notation, mainly because it has been used previously in that form; however, similar limitations also apply for this variable.

Another potential source of uncertainty is the limited quality of sampling of the phase space related to the reaction, as presently reflected in the snapshots. Sampling of the phase space of enzymatic reactions poses a long-standing problem,⁵⁴ because the chemical coordinate and the enzyme's degrees of freedom are coupled. Consequently, substantial torsional displacements of the side chains and large-amplitude fluctuations of the tertiary structure of the protein may have considerable impacts on the catalytic effect, but the time scale at which these fluctuations occur often prevents them from being sampled adequately. For the simulation of the presently studied reaction⁶⁰ it was necessary to restrain torsional flexibility of the reacting moiety in order to obtain smooth free energy profiles at the simulation time scale of up to tens of nanoseconds.⁹² A more flexible model would require significantly longer simulations (possibly microseconds or longer) and would be prohibitively expensive.

A challenge for future work is to generalize the findings about the important role of electrostatics in the catalytic function of MAO A to other enzymes, requiring broad investigation of different enzymes and their reactions.

■ ASSOCIATED CONTENT

§ Supporting Information

The Supporting Information is available free of charge on the ACS Publications website at DOI: 10.1021/acscatal.8b04045.

Details of the reaction mechanism, simulation of the catalytic step, electric field calculation descriptions, additional explanations and clarifications, table of individual residue contributions to $\Delta G_{\text{elec}}^\ddagger(x)$ (PDF)

■ AUTHOR INFORMATION

Corresponding Author

*E-mail: jernej.stare@ki.si.

ORCID

Jernej Stare: 0000-0002-2018-6688

Present Address

[§]E.F.: Department of Pharmacy, Faculty of Health and Medical Sciences, University of Copenhagen, 2200 Copenhagen, Denmark.

Notes

The authors declare no competing financial interest.

■ ACKNOWLEDGMENTS

This work benefited from the program funding of the Slovenian Research Agency (codename P1-0012) as well as from the young researchers grant awarded to A.P.

■ REFERENCES

- (1) Shaw, D. E. Anton: A Specialized Machine for Millisecond-Scale Molecular Dynamics Simulations of Proteins. *2009 19th IEEE Int. Symp. Computer Arithmetic* **2009**, 0, 3.
- (2) Grossman, J. P.; Towles, B.; Greskamp, B.; Shaw, D. E. Filtering, Reductions and Synchronization in the Anton 2 Network. *2015 IEEE 29th Int. Par. and Distr. Processing Symp.* **2015**, 0, 860–870.
- (3) Lindorff-Larsen, K.; Piana, S.; Dror, R. O.; Shaw, D. E. How Fast-Folding Proteins Fold. *Science* **2011**, 334, 517–520.
- (4) Shaw, D. E.; Maragakis, P.; Lindorff-Larsen, K.; Piana, S.; Dror, R. O.; Eastwood, M. P.; Bank, J. A.; Jumper, J. M.; Salmon, J. K.; Shan, Y. B.; Wriggers, W. Atomic-Level Characterization of the Structural Dynamics of Proteins. *Science* **2010**, 330, 341–346.
- (5) Warshel, A.; Sharma, P. K.; Kato, M.; Xiang, Y.; Liu, H. B.; Olsson, M. H. M. Electrostatic Basis for Enzyme Catalysis. *Chem. Rev.* **2006**, 106, 3210–3235.
- (6) Bar-Even, A.; Noor, E.; Savir, Y.; Liebermeister, W.; Davidi, D.; Tawfik, D. S.; Milo, R. The Moderately Efficient Enzyme: Evolutionary and Physicochemical Trends Shaping Enzyme Parameters. *Biochemistry* **2011**, 50, 4402–4410.
- (7) Pauling, L. Molecular Architecture and Biological Reactions. *Chem. Eng. News* **1946**, 24, 1375–1377.
- (8) Warshel, A.; Levitt, M. Theoretical Studies of Enzymic Reactions - Dielectric, Electrostatic and Steric Stabilization of Carbonium-Ion in Reaction of Lysozyme. *J. Mol. Biol.* **1976**, 103, 227–249.
- (9) Singh, U. C.; Kollman, P. A. A Combined Abinitio Quantum-Mechanical and Molecular Mechanical Method for Carrying out Simulations on Complex Molecular-Systems - Applications to the CH₃Cl + Cl⁻ Exchange-Reaction and Gas-Phase Protonation of Polyethers. *J. Comput. Chem.* **1986**, 7, 718–730.
- (10) Bash, P. A.; Field, M. J.; Karplus, M. Free-Energy Perturbation Method for Chemical-Reactions in the Condensed Phase - a Dynamical-Approach Based on a Combined Quantum and Molecular Mechanics Potential. *J. Am. Chem. Soc.* **1987**, 109, 8092–8094.
- (11) Brunk, E.; Rothlisberger, U. Mixed Quantum Mechanical/Molecular Mechanical Molecular Dynamics Simulations of Biological Systems in Ground and Electronically Excited States. *Chem. Rev.* **2015**, 115, 6217–6263.

- (12) Acevedo, O.; Jorgensen, W. L. Advances in Quantum and Molecular Mechanical (QM/MM) Simulations for Organic and Enzymatic Reactions. *Acc. Chem. Res.* **2010**, *43*, 142–151.
- (13) Chandrasekhar, J.; Smith, S. F.; Jorgensen, W. L. SN2 Reaction Profiles in the Gas-Phase and Aqueous-Solution. *J. Am. Chem. Soc.* **1984**, *106*, 3049–3050.
- (14) Jorgensen, W. L. Free-Energy Calculations - a Breakthrough for Modeling Organic-Chemistry in Solution. *Acc. Chem. Res.* **1989**, *22*, 184–189.
- (15) Warshel, A. Electrostatic Origin of the Catalytic Power of Enzymes and the Role of Preorganized Active Sites. *J. Biol. Chem.* **1998**, *273*, 27035–27038.
- (16) Warshel, A. Energetics of Enzyme Catalysis. *Proc. Natl. Acad. Sci. U. S. A.* **1978**, *75*, 5250–5254.
- (17) Warshel, A. Electrostatic Basis of Structure-Function Correlation in Proteins. *Acc. Chem. Res.* **1981**, *14*, 284–290.
- (18) Warshel, A.; Aqvist, J.; Creighton, S. Enzymes Work by Solvation Substitution Rather Than by Desolvation. *Proc. Natl. Acad. Sci. U. S. A.* **1989**, *86*, 5820–5824.
- (19) Cannon, W. R.; Singleton, S. F.; Benkovic, S. J. A Perspective on Biological Catalysis. *Nat. Struct. Mol. Biol.* **1996**, *3*, 821–833.
- (20) Antoniou, D.; Schwartz, S. D. Large Kinetic Isotope Effects in Enzymatic Proton Transfer and the Role of Substrate Oscillations. *Proc. Natl. Acad. Sci. U. S. A.* **1997**, *94*, 12360–12365.
- (21) Kohen, A.; Cannio, R.; Bartolucci, S.; Klinman, J. P. Enzyme Dynamics and Hydrogen Tunnelling in a Thermophilic Alcohol Dehydrogenase. *Nature* **1999**, *399*, 496–499.
- (22) Eisenmesser, E. Z.; Bosco, D. A.; Akke, M.; Kern, D. Enzyme Dynamics During Catalysis. *Science* **2002**, *295*, 1520–1523.
- (23) Nam, K.; Prat-Resina, X.; Garcia-Viloca, M.; Devi-Kesavan, L. S.; Gao, J. Dynamics of an Enzymatic Substitution Reaction in Haloalkane Dehalogenase. *J. Am. Chem. Soc.* **2004**, *126*, 1369–1376.
- (24) Henzler-Wildman, K. A.; Thai, V.; Lei, M.; Ott, M.; Wolf-Watz, M.; Fenn, T.; Pozharski, E.; Wilson, M. A.; Petsko, G. A.; Karplus, M.; Hubner, C. G.; Kern, D. Intrinsic Motions Along an Enzymatic Reaction Trajectory. *Nature* **2007**, *450*, 838–844.
- (25) Hay, S.; Scrutton, N. S. Good Vibrations in Enzyme-Catalysed Reactions. *Nat. Chem.* **2012**, *4*, 161–168.
- (26) Agarwal, P. K.; Billeter, S. R.; Rajagopalan, P. T. R.; Benkovic, S. J.; Hammes-Schiffer, S. Network of Coupled Promoting Motions in Enzyme Catalysis. *Proc. Natl. Acad. Sci. U. S. A.* **2002**, *99*, 2794–2799.
- (27) Glowacki, D. R.; Harvey, J. N.; Mulholland, A. J. Taking Ockham's Razor to Enzyme Dynamics and Catalysis. *Nat. Chem.* **2012**, *4*, 169–176.
- (28) Tunon, I.; Laage, D.; Hynes, J. T. Are There Dynamical Effects in Enzyme Catalysis? Some Thoughts Concerning the Enzymatic Chemical Step. *Arch. Biochem. Biophys.* **2015**, *582*, 42–55.
- (29) Kamerlin, S. C. L.; Warshel, A. At the Dawn of the 21st Century: Is Dynamics the Missing Link for Understanding Enzyme Catalysis? *Proteins: Struct., Funct., Genet.* **2010**, *78*, 1339–1375.
- (30) Warshel, A.; Bora, R. P. Perspective: Defining and Quantifying the Role of Dynamics in Enzyme Catalysis. *J. Chem. Phys.* **2016**, *144*, 180901–1–17.
- (31) Hammes-Schiffer, S. Catalytic Efficiency of Enzymes: A Theoretical Analysis. *Biochemistry* **2013**, *52*, 2012–2020.
- (32) Olsson, M. H. M.; Parson, W. W.; Warshel, A. Dynamical Contributions to Enzyme Catalysis: Critical Tests of a Popular Hypothesis. *Chem. Rev.* **2006**, *106*, 1737–1756.
- (33) Luk, L. Y.; Ruiz-Pernia, J. J.; Adesina, A. S.; Loveridge, E. J.; Tunon, I.; Moliner, V.; Allemann, R. K. Chemical Ligation and Isotope Labeling to Locate Dynamic Effects During Catalysis by Dihydrofolate Reductase. *Angew. Chem., Int. Ed.* **2015**, *54*, 9016–9020.
- (34) Luk, L. Y.; Loveridge, E. J.; Allemann, R. K. Protein Motions and Dynamic Effects in Enzyme Catalysis. *Phys. Chem. Chem. Phys.* **2015**, *17*, 30817–30827.
- (35) Nagel, Z. D.; Klinman, J. P. A 21st Century Revisionist's View at a Turning Point in Enzymology. *Nat. Chem. Biol.* **2009**, *5*, 543–550.
- (36) Bhowmick, A.; Sharma, S. C.; Head-Gordon, T. The Importance of the Scaffold for De Novo Enzymes: A Case Study with Kemp Eliminase. *J. Am. Chem. Soc.* **2017**, *139*, 5793–5800.
- (37) Vaissier, V.; Sharma, S. C.; Schaettle, K.; Zhang, T.; Head-Gordon, T. Computational Optimization of Electric Fields for Improving Catalysis of a Designed Kemp Eliminase. *ACS Catal.* **2018**, *8*, 219–227.
- (38) Shaik, S.; de Visser, S. P.; Kumar, D. External Electric Field Will Control the Selectivity of Enzymatic-Like Bond Activations. *J. Am. Chem. Soc.* **2004**, *126*, 11746–11749.
- (39) Hirao, H.; Chen, H.; Carvajal, M. A.; Wang, Y.; Shaik, S. Effect of External Electric Fields on the C-H Bond Activation Reactivity of Nonheme Iron-Oxo Reagents. *J. Am. Chem. Soc.* **2008**, *130*, 3319–3327.
- (40) Shaik, S.; Mandal, D.; Ramanan, R. Oriented Electric Fields as Future Smart Reagents in Chemistry. *Nat. Chem.* **2016**, *8*, 1091–1098.
- (41) Wang, Z. F.; Danovich, D.; Ramanan, R.; Shaik, S. Oriented-External Electric Fields Create Absolute Enantioselectivity in Diels-Alder Reactions: Importance of the Molecular Dipole Moment. *J. Am. Chem. Soc.* **2018**, *140*, 13350–13359.
- (42) Shaik, S.; Ramanan, R.; Danovich, D.; Mandal, D. Structure and Reactivity/Selectivity Control by Oriented-External Electric Fields. *Chem. Soc. Rev.* **2018**, *47*, 5125–5145.
- (43) Lai, W.; Chen, H.; Cho, K.-B.; Shaik, S. External Electric Field Can Control the Catalytic Cycle of Cytochrome P450cam: A QM/MM Study. *J. Phys. Chem. Lett.* **2010**, *1*, 2082–2087.
- (44) Welborn, V. V.; Ruiz Pestana, L.; Head-Gordon, T. Computational Optimization of Electric Fields for Better Catalysis Design. *Nat. Catal.* **2018**, *1*, 649–655.
- (45) Klinska, M.; Smith, L. M.; Gryn'ova, G.; Banwell, M. G.; Coote, M. L. Experimental Demonstration of pH-Dependent Electrostatic Catalysis of Radical Reactions. *Chem. Sci.* **2015**, *6*, 5623–5627.
- (46) Aragones, A. C.; Haworth, N. L.; Darwish, N.; Ciampi, S.; Bloomfield, N. J.; Wallace, G. G.; Diez-Perez, I.; Coote, M. L. Electrostatic Catalysis of a Diels-Alder Reaction. *Nature* **2016**, *531*, 88–91.
- (47) Ciampi, S.; Darwish, N.; Aitken, H. M.; Diez-Perez, I.; Coote, M. L. Harnessing Electrostatic Catalysis in Single Molecule, Electrochemical and Chemical Systems: A Rapidly Growing Experimental Tool Box. *Chem. Soc. Rev.* **2018**, *47*, 5146–5164.
- (48) Fried, S. D.; Boxer, S. G. Electric Fields and Enzyme Catalysis. *Annu. Rev. Biochem.* **2017**, *86*, 387–415.
- (49) Fried, S. D.; Bagchi, S.; Boxer, S. G. Extreme Electric Fields Power Catalysis in the Active Site of Ketosteroid Isomerase. *Science* **2014**, *346*, 1510–1514.
- (50) Zoi, I.; Antoniou, D.; Schwartz, S. D. Electric Fields and Fast Protein Dynamics in Enzymes. *J. Phys. Chem. Lett.* **2017**, *8*, 6165–6170.
- (51) Morgenstern, A.; Jaszai, M.; Eberhart, M. E.; Alexandrova, A. N. Quantified Electrostatic Preorganization in Enzymes Using the Geometry of the Electron Charge Density. *Chem. Sci.* **2017**, *8*, 5010–5018.
- (52) Repič, M.; Purg, M.; Vianello, R.; Mavri, J. Examining Electrostatic Preorganization in Monoamine Oxidases A and B by Structural Comparison and pKa Calculations. *J. Phys. Chem. B* **2014**, *118*, 4326–4332.
- (53) Schyman, P.; Lai, W. Z.; Chen, H.; Wang, Y.; Shaik, S. The Directive of the Protein: How Does Cytochrome P450 Select the Mechanism of Dopamine Formation? *J. Am. Chem. Soc.* **2011**, *133*, 7977–7984.
- (54) Bolhuis, P. G.; Chandler, D.; Dellago, C.; Geissler, P. L. Transition Path Sampling: Throwing Ropes over Rough Mountain Passes, in the Dark. *Annu. Rev. Phys. Chem.* **2002**, *53*, 291–318.
- (55) Laio, A.; Parrinello, M. Escaping Free-Energy Minima. *Proc. Natl. Acad. Sci. U. S. A.* **2002**, *99*, 12562–12566.
- (56) Huber, T.; Torda, A. E.; Vangunsteren, W. F. Local Elevation - a Method for Improving the Searching Properties of Molecular-Dynamics Simulation. *J. Comput.-Aided Mol. Des.* **1994**, *8*, 695–708.

- (57) Torrie, G. M.; Valleau, J. P. Non-Physical Sampling Distributions in Monte-Carlo Free-Energy Estimation - Umbrella Sampling. *J. Comput. Phys.* **1977**, *23*, 187–199.
- (58) Zwanzig, R. W. High Temperature Equation of State by a Perturbation Method. I. Nonpolar Gases. *J. Chem. Phys.* **1954**, *22*, 1420–1426.
- (59) Kollman, P. Free-Energy Calculations - Applications to Chemical and Biochemical Phenomena. *Chem. Rev.* **1993**, *93*, 2395–2417.
- (60) Oanca, G.; Purg, M.; Mavri, J.; Shih, J. C.; Stare, J. Insights into Enzyme Point Mutation Effect by Molecular Simulation: Phenylethylamine Oxidation Catalyzed by Monoamine Oxidase A. *Phys. Chem. Chem. Phys.* **2016**, *18*, 13346–13356.
- (61) Shih, J. C.; Chen, K.; Ridd, M. J. Monoamine Oxidase: From Genes to Behavior. *Annu. Rev. Neurosci.* **1999**, *22*, 197–217.
- (62) Bortolato, M.; Chen, K.; Shih, J. C. Monoamine Oxidase Inactivation: From Pathophysiology to Therapeutics. *Adv. Drug Delivery Rev.* **2008**, *60*, 1527–1533.
- (63) Brunner, H. G.; Nelen, M.; Breakefield, X. O.; Ropers, H. H.; Vanoost, B. A. Abnormal-Behavior Associated with a Point Mutation in the Structural Gene for Monoamine Oxidase A. *Science* **1993**, *262*, 578–580.
- (64) Pivac, N.; Knezevic, J.; Kozaric-Kovacic, D.; Dezeljin, M.; Mustapic, M.; Rak, D.; Matijevic, T.; Pavelic, J.; Muck-Seler, D. Monoamine Oxidase (MAO) Intron 13 Polymorphism and Platelet MAO-B Activity in Combat-Related Posttraumatic Stress Disorder. *J. Affective Disord.* **2007**, *103*, 131–138.
- (65) Cases, O.; Seif, I.; Grimsby, J.; Gaspar, P.; Chen, K.; Pournin, S.; Muller, U.; Aguet, M.; Babinet, C.; Shih, J. C.; Demaeyer, E. Aggressive-Behavior and Altered Amounts of Brain-Serotonin and Norepinephrine in Mice Lacking MAOA. *Science* **1995**, *268*, 1763–1766.
- (66) Szabo, A.; Billett, E.; Turner, J. Phenylethylamine, a Possible Link to the Antidepressant Effects of Exercise? *Br. J. Sports Med.* **2001**, *35*, 342–343.
- (67) Janssen, P. A. J.; Leysen, O. E.; Megens, A. A. H. P.; Awouters, F. H. L. Does Phenylethylamine Act as an Endogenous Amphetamine in Some Patients? *Int. J. Neuropsychopharmacol.* **1999**, *2*, 229–240.
- (68) Wolf, M. E.; Mesnaim, A. D. Phenylethylamine in Neuropsychiatric Disorders. *Gen. Pharmacol.* **1983**, *14*, 385–390.
- (69) Zenn, R. K.; Abad, E.; Kastner, J. Influence of the Environment on the Oxidative Deamination of P-Substituted Benzylamines in Monoamine Oxidase. *J. Phys. Chem. B* **2015**, *119*, 3678–3686.
- (70) Geha, R. M.; Rebrin, I.; Chen, K.; Shih, J. C. Substrate and Inhibitor Specificities for Human Monoamine Oxidase A and B Are Influenced by a Single Amino Acid. *J. Biol. Chem.* **2001**, *276*, 9877–9882.
- (71) Tan, A. K.; Ramsay, R. R. Substrate-Specific Enhancement of the Oxidative Half-Reaction of Monoamine-Oxidase. *Biochemistry* **1993**, *32*, 2137–2143.
- (72) Nandigama, R.; Edmondson, D. Structure-Activity Relations in the Oxidation of Phenethylamine Analogues by Recombinant Human Liver Monoamine Oxidase A. *Biochemistry* **2000**, *39*, 15258–15265.
- (73) Vianello, R.; Repič, M.; Mavri, J. How Are Biogenic Amines Metabolized by Monoamine Oxidases? *Eur. J. Org. Chem.* **2012**, *2012* (36), 7057–7065.
- (74) Zapata-Torres, G.; Fierro, A.; Barriga-Gonzalez, G.; Salgado, J. C.; Celis-Barros, C. Revealing Monoamine Oxidase B Catalytic Mechanisms by Means of the Quantum Chemical Cluster Approach. *J. Chem. Inf. Model.* **2015**, *55*, 1349–1360.
- (75) Aqvist, J.; Warshel, A. Simulation of Enzyme-Reactions Using Valence-Bond Force-Fields and Other Hybrid Quantum-Classical Approaches. *Chem. Rev.* **1993**, *93*, 2523–2544.
- (76) Warshel, A.; Weiss, R. M. An Empirical Valence Bond Approach for Comparing Reactions in Solutions and in Enzymes. *J. Am. Chem. Soc.* **1980**, *102*, 6218–6226.
- (77) Barone, V.; Cossi, M. Quantum Calculation of Molecular Energies and Energy Gradients in Solution by a Conductor Solvent Model. *J. Phys. Chem. A* **1998**, *102*, 1995–2001.
- (78) Cossi, M.; Rega, N.; Scalmani, G.; Barone, V. Energies, Structures, and Electronic Properties of Molecules in Solution with the C-PCM Solvation Model. *J. Comput. Chem.* **2003**, *24*, 669–681.
- (79) Glendening, E. D.; Reed, A. E.; Carpenter, J. E.; Weinhold, F. NBO, version 3.1; University of Wisconsin: Madison, WI, USA, 2001.
- (80) Singh, U. C.; Kollman, P. A. An Approach to Computing Electrostatic Charges for Molecules. *J. Comput. Chem.* **1984**, *5*, 129–145.
- (81) Frisch, M. J.; Trucks, G. W.; Schlegel, H. B.; Scuseria, G. E.; Robb, M. A.; Cheeseman, J. R.; Scalmani, G.; Barone, V.; Mennucci, B.; Petersson, G. A.; Nakatsuji, H.; Caricato, M.; Li, X.; Hratchian, H. P.; Izmaylov, A. F.; Bloino, J.; Zheng, G.; Sonnenberg, J. L.; Hada, M.; Ehara, M.; Toyota, K.; Fukuda, R.; Hasegawa, J.; Ishida, M.; Nakajima, T.; Honda, Y.; Kitao, O.; Nakai, H.; Vreven, T.; Montgomery, J. A., Jr.; Peralta, J. E.; Ogliaro, F.; Bearpark, M. J.; Heyd, J.; Brothers, E. N.; Kudin, K. N.; Staroverov, V. N.; Kobayashi, R.; Normand, J.; Raghavachari, K.; Rendell, A. P.; Burant, J. C.; Iyengar, S. S.; Tomasi, J.; Cossi, M.; Rega, N.; Millam, N. J.; Klene, M.; Knox, J. E.; Cross, J. B.; Bakken, V.; Adamo, C.; Jaramillo, J.; Gomperts, R.; Stratmann, R. E.; Yazyev, O.; Austin, A. J.; Cammi, R.; Pomelli, C.; Ochterski, J. W.; Martin, R. L.; Morokuma, K.; Zakrzewski, V. G.; Voth, G. A.; Salvador, P.; Dannenberg, J. J.; Dapprich, S.; Daniels, A. D.; Farkas, Ö.; Foresman, J. B.; Ortiz, J. V.; Cioslowski, J.; Fox, D. J. *Gaussian 09*; Gaussian, Inc.: Wallingford, CT, USA, 2009.
- (82) Humphrey, W.; Dalke, A.; Schulten, K. VMD: Visual Molecular Dynamics. *J. Mol. Graphics* **1996**, *14*, 33–38.
- (83) Poberžnik, M.; Purg, M.; Repič, M.; Mavri, J.; Vianello, R. Empirical Valence Bond Simulations of the Hydride-Transfer Step in the Monoamine Oxidase A Catalyzed Metabolism of Noradrenaline. *J. Phys. Chem. B* **2016**, *120*, 11419–11427.
- (84) Abad, E.; Zenn, R. K.; Kastner, J. Reaction Mechanism of Monoamine Oxidase from QM/MM Calculations. *J. Phys. Chem. B* **2013**, *117*, 14238–14246.
- (85) Akyuz, M. A.; Erdem, S. S. Computational Modeling of the Direct Hydride Transfer Mechanism for the MAO Catalyzed Oxidation of Phenethylamine and Benzylamine: ONIOM (QM/QM) Calculations. *J. Neural Transm.* **2013**, *120*, 937–945.
- (86) Atalay, V. E.; Erdem, S. S. A Comparative Computational Investigation on the Proton and Hydride Transfer Mechanisms of Monoamine Oxidase Using Model Molecules. *Comput. Biol. Chem.* **2013**, *47*, 181–191.
- (87) Fitzpatrick, P. F. Oxidation of Amines by Flavoproteins. *Arch. Biochem. Biophys.* **2010**, *493*, 13–25.
- (88) Akyüz, M. A.; Erdem, S. S.; Edmondson, D. E. The Aromatic Cage in the Active Site of Monoamine Oxidase B: Effect on the Structural and Electronic Properties of Bound Benzylamine and P-Nitrobenzylamine. *J. Neural Transm.* **2007**, *114*, 693–698.
- (89) Fried, S. D.; Boxer, S. G. Measuring Electric Fields and Noncovalent Interactions Using the Vibrational Stark Effect. *Acc. Chem. Res.* **2015**, *48*, 998–1006.
- (90) Suydam, I. T.; Snow, C. D.; Pande, V. S.; Boxer, S. G. Electric Fields at the Active Site of an Enzyme: Direct Comparison of Experiment with Theory. *Science* **2006**, *313*, 200–204.
- (91) Suydam, I. T.; Boxer, S. G. Vibrational Stark Effects Calibrate the Sensitivity of Vibrational Probes for Electric Fields in Proteins. *Biochemistry* **2003**, *42*, 12050–12055.
- (92) Stare, J. Complete Sampling of an Enzyme Reaction Pathway: A Lesson from Gas Phase Simulations. *RSC Adv.* **2017**, *7*, 8740–8754.